Science of the Total Environment 626 (2018) 567–580

Contents lists available at ScienceDirect

Science of the Total Environment

journal homepage: www.elsevier.com/locate/scitotenv

Identifying outdoor thermal risk areas and evaluation of future thermal comfort concerning shading orientation in a traditional settlement

Kuo-Tsang Huang [a], Shing-Ru Yang [b], Andreas Matzarakis [c,d], Tzu-Ping Lin [b,*]

[a] Department of Bioenvironmental Systems Engineering, National Taiwan University, 1 Sec. 4, Roosevelt Rd., Taipei 106, Taiwan
[b] Department of Architecture, National Cheng Kung University, 1 University Rd., East Dist., Tainan 701, Taiwan
[c] Research Center Human Biometeorology, German Meteorological Service, D-79104 Freiburg, Germany
[d] Chair of Environmental Meteorology, Faculty of Environment and Natural Resources, Albert-Ludwigs-University Freiburg, Germany.

HIGHLIGHTS

- Hazard, exposure and vulnerability aspects were assessed to identify thermal risk in a traditional settlement in hot-and-humid Tainan, Taiwan.
- Hourly future climate data were constructed based on morphing method with GCM.
- Thermal stress map was produced by ENVI-met and future thermal comfort was simulated by RayMan.
- Maximum estimation of 168% increment of high outdoor thermal risk in the far future

GRAPHICAL ABSTRACT

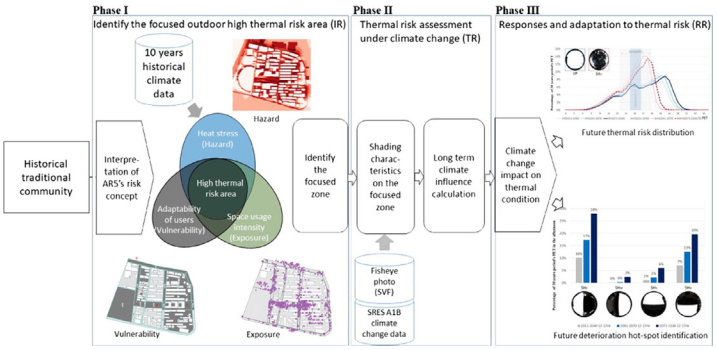
Phase I
Identify the focused outdoor high thermal risk area (IR)
Phase II
Thermal risk assessment under climate change (TR)
Phase III
Responses and adaptation to thermal risk (RR)
10 years historical climate data
Hazard
Historical traditional community
Interpre-tation of AR5's risk concept
Heat stress (Hazard)
High thermal risk area
Adaptability of users (Vulnerability)
Space usage intensity (Exposure)
Identify the focused zone
Shading charac-teristics on the focused zone
Long term climate influence calculation
Climate change impact on thermal condition
Future thermal risk distribution
Fisheye photo (SVF)
SRES A1B climate change data
Vulnerability
Exposure
Future deterioration hot-spot identification

ARTICLE INFO

Article history:
Received 29 September 2017
Received in revised form 5 December 2017
Accepted 4 January 2018
Available online 19 February 2018

Editor: SCOTT SHERIDAN

Keywords:
Outdoor thermal comfort
Thermal stress risk identification
Future climate
Taiwan

ABSTRACT

The outdoor thermal environment is expected to be deteriorated under climate change. An approach of risk identification including assessment from aspects of thermal stress effect, people's exposure, and local's vulnerability were adopted to study a hot-and-humid traditional rural community located at Tainan, Taiwan. Layers of each aspect were either constructed by in-situ measurements or simulations. To evaluate the future thermal comfort changes by simulations, the prerequisite hourly climate data of three future time slices were produced. Prognostic simulation model, ENVI-met, in combination with diagnostic model, RayMan, were respectively used for identifying current spatial distribution of thermal stress and for assessing the future thermal comfort changes. High thermal risk area was identified by superimposing layers of hazard, exposure and vulnerability. It revealed that because of the tourists' vulnerability to adapt local climate and the inflexibleness of choosing visiting time, it exhibited a high thermal stress at the Main Courtyard where its thermal comfort conditions will be deteriorated due to climate change. Furthermore, the thermal comfort conditions in various shading orientation were analyzed based on the changing climate in three future time slices, i.e. 2011–2040, 2041–2070, and 2071–2100. The results show the area with shading in the East and West side is more comfort than in the North side. In hot season, shading in the West side contributes less PET increasing, especially in the afternoon period. The severest overheat problem (the physiological equivalent temperature, PET > 40 °C) at the Main Courtyard will increase from current 10% to 28% in 2071–2100 in terms of overheating occurrence frequency. The results of this study can be used as the guidelines for environment analysis before planning or redesign community.

© 2018 Elsevier B.V. All rights reserved.

* Corresponding author.
E-mail address: lintp@mail.ncku.edu.tw (T.-P. Lin).

https://doi.org/10.1016/j.scitotenv.2018.01.031
0048-9697/© 2018 Elsevier B.V. All rights reserved.

1. Introduction

Anthropogenic activities would increase the emission of carbon dioxide resulting future climate change according to the report proposed by the Intergovernmental Panel on Climate Change (IPCC) in 2014 (IPCC, 2014). Previous study reveals that outdoor thermal environment perceived by a person will be affected by outdoor climate and the built environment (Lin et al., 2010). Less appropriate environmental design would also influence the conditions of microclimate and hence may jeopardize the thermal comfort. Therefore, how to formulate outdoor environmental design/planning by evaluating the outdoor thermal conditions under the context of climate change is the primary issue in this study.

Previous outdoor thermal comfort studies related to climate change are focused on outdoor environmental evaluation in perspective of urban context (Norton et al., 2015; Ren et al., 2012) or in terms of social-economic disaster mitigation (Csete et al., 2013; Moreno and Becken, 2009). Many thermal environmental studies aimed at community scale using climate change data for thermal environment simulation (Conry et al., 2015; Gromke et al., 2015; Lau et al., 2015; Loughnan et al., 2015; Peng and Elwan, 2014; Skelhorn et al., 2014), or performing comparisons between the measured and the simulated results (Cheung and Hart, 2014; Matzarakis and Endler, 2010; Muthers et al., 2010; Scott et al., 2015; Yang et al., 2015), or analyzing the actual environment with the observed and simulated meteorological data (Chen and Ng, 2011; Kuwae et al., 2004; Wang and Akbari, 2014). For those studies focusing on the issues of outdoor environment, the methods used by most researches are utilizing weather information, either measured or simulated, to discuss with shading ratio (Höppe, 1999; IPCC, 2000; Kruger et al., 2014; Lee et al., 2014; Lin et al., 2013b; Noro et al., 2015), human moving behaviors (Kantor and Unger, 2010; Nikolopoulou and Lykoudis, 2007), or with the thermal comfort of human body (Brosy et al., 2014; Lin and Matzarakis, 2008; Loughnan et al., 2015; Yang et al., 2013a; Yin et al., 2012).

Several studies regarding outdoor thermal comfort had been done in Taiwan: Hwang and Lin established the outdoor thermal comfort range for Taiwanese people (Hwang and Lin, 2007). Afterwards, outdoor thermal comfort studies and investigations focused on public square (Huang et al., 2015; Lin, 2009), urban parks (Lin et al., 2013a), school campus (Shih et al., 2017), and a rural traditional settlement (Yang and Lin, 2016) were extensively conducted based on the current climate conditions. However, the ambient air temperature increase rate of 0.81 °C per 25 years is observed in Tainan plain area under the influence of climate change (Lin et al., 2015). Another study on future urban heat island intensity (UHII) variation projection in central Taiwan area indicates that the UHII will increase to a maximum of 5.8 °C during 2075–2099 and, accordingly, will result in 476.9% increase in residential cooling energy use (Hwang et al., 2017). Furthermore, Lin et al. used the wet-bulb globe temperature index (WBGT) to evaluate future outdoor heat stress condition and found that it will be at danger level (WBGT > 31 °C) in summer months at the end of the 21st Century (Lin et al., 2017). All these studies show an imperative need to evaluate future outdoor thermal environment variation and formulate adaptation strategies to improve outdoor thermal comfort in facing with the changing climate to help resilience at community level.

The constraints of existing studies are as follows:

Firstly, none existing thermal environmental studies have analyzed both human usage behavior and their adaptability to the space. Many researches use single thermal index, such as physiologically equivalent temperature (PET) (VDI, 1998), to evaluate thermal conditions and user's adaptation of a given space regardless of the information such as the allocation and the degree of heat stress endurance of the space users. The understanding of the effect the micro-climate has on to a human is limited.

Secondly, single simulation tool cannot effectively fully demonstrate spatial and temporal distribution of micro-climate. Previous studies usually use one certain simulation tool as a method for evaluating outdoor thermal stress (Peng and Elwan, 2014), which it exhibits several limitations. Take general prognostic simulation tools (Loughnan et al., 2015; Yang et al., 2013a) for example, although spatial distribution of thermal conditions can be predicted and illustrated, due to computational constraints, it is not viable for presenting the thermal conditions results for a prolonged period of time. In contrast, although MRT of a given location point can be rapidly estimated by means of diagnostic model, such as RayMan model (Matzarakis et al., 2007a; Matzarakis et al., 2010), it is not capable for calculating spatial distribution of MRT across vast areas.

Thirdly, only thermal environment improvement of a given area is proposed in previous studies. A general hypothesis of the usage of a given space in previous studies is it always assumed that the human behavior is identical and is independent of time and the number of users, which usually results in proposing a universal layout design or material usage suggestions, such as increasing the greenery or changing the pavement material etc. (Matzarakis and Endler, 2010; Muthers et al., 2010). However, there are spaces where seldom people will use and is needless to be improved; or there are spaces where people will use during a specific time period or will be only gathered by certain groups of people. The adequate adaptation strategies should carefully be proposed by additionally considering the above different usage demands and limitations. By this means the adaptation strategies can be appropriately proposed and are able to be conveniently implemented to confront the impact of the changing climate.

Therefore, the objectives of this study in corresponding to the above three raised issues are:

1) To identify outdoor high thermal heat stress area in perspective of micro-climate risk assessment,
2) To evaluate thermal comfort condition in the thermal risk area based on various shading orientation, and.
3) To quantify daily, seasonal, and annually thermal stress condition and frequencies based on the future climate data.

2. Method

2.1. Research structure

To investigate the effect of climate change and the possible adaptation measures in terms of outdoor thermal risk, we followed the risk concept given in IPCC's the fifth assessment report (AR5). A previous study also adopted IPCC's risk assessment concept from hazard, vulnerability, and exposure perspectives in proposing a framework on the prioritization of green infrastructure allocation to alleviate UHI (Norton et al., 2015).

The research structure is as Fig. 1. In the first phase (IR) we firstly reinterpret the definition of hazard, exposure and vulnerability defined in IPCC AR5 to correspond to the assessment frame of local thermal for identifying the high thermal risk hot-spot in the studied community. The recognized hot-spot areas are the one we must prior focus on. In the second phase (TR), the existing outdoor shading locations in the hot-spot area were analyzed with the future weather data to investigate the influences on thermal comfort due to climate change. In the third phase (RR), the corresponding responses and adaptation measures were proposed in terms of hazard, exposure and vulnerability framework.

2.2. In-situ measurement and the environmental analytic tool

2.2.1. Investigation target and the research method

The research location is at Lutaoyang (N23°00′, E120°12′), where it is a historical traditional settlement in Tainan's suburban area with the altitude being 100 m, comprising about 3.4 ha with 160 m wide and 210 m long. The geographic location is as Fig. 2. Lutaoyang, where is a

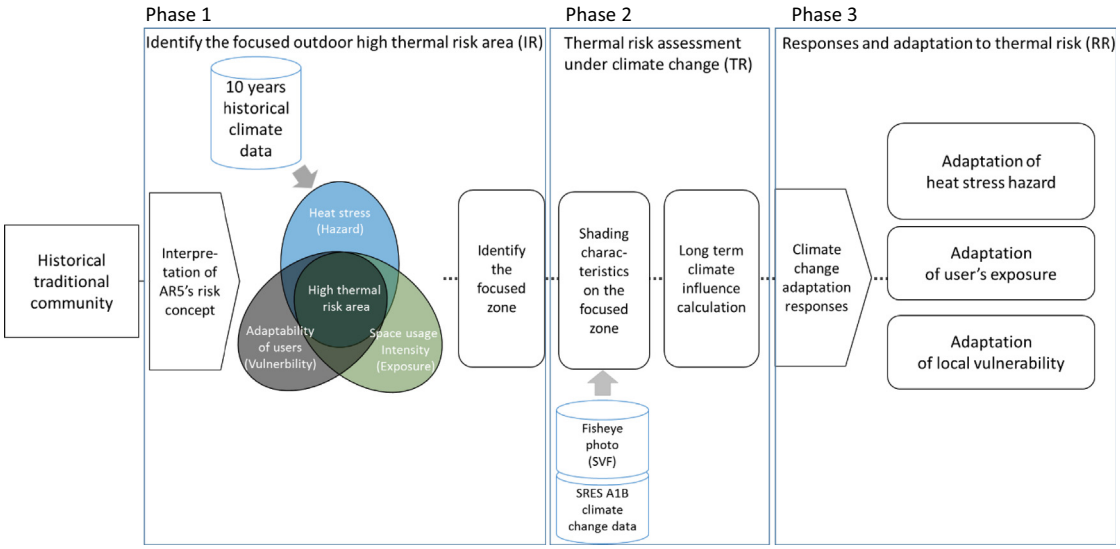
Phase 1
Identify the focused outdoor high thermal risk area (IR)
Phase 2
Thermal risk assessment under climate change (TR)
Phase 3
Responses and adaptation to thermal risk (RR)
10 years historical climate data
Historical traditional community
Interpre-tation of AR5's risk concept
Heat stress (Hazard)
High thermal risk area
Adaptability of users (Vulnerbility)
Space usage intensity (Exposure)
Identify the focused zone
Shading charac-teristics on the focused zone
Long term climate influence calculation
Fisheye photo (SVF)
SRES A1B climate change data
Climate change adaptation responses
Adaptation of heat stress hazard
Adaptation of user's exposure
Adaptation of local vulnerability

Fig. 1. The structure of the research (Phase 1 (IR): identify the focused outdoor high thermal risk area; phase 2 (TR):thermal risk assessment under climate change; phase 3 (RR): responses and adaptation to the thermal risk).

thriving tourist destination, is a traditional tribal community officially recognized by Taiwan's Ministry of Culture, and is the largest single surname settlement ("Jiang") in Taiwan. The annual average temperature is 24.1 °C with the monthly average being 17.4 °C in the coldest month January and is 29.0 °C in the hottest month July. The prevailing wind in summer is from southwest.

A total of 18 in-situ measurement points were selected throughout the community. The air temperature, air humidity and globe temperature of each point were long-term monitored and recorded with an interval of 1 min from 8:00–17:00 on a typical day of a given month during November 2013 to October 2014. The data logger used therein was Center314 with a recording resolution of ±0.1 °C for dry-bulb temperature, ±0.5 °C for globe temperature and ±2.5% for relative humidity (Yang and Lin, 2016). The outdoor measurement locations were chosen based on having various degrees of shading in both tourism spots and local residents' daily

Fig. 2. (a) The geographic location of the traditional rural community, Lutaoyang. (b) Satellite image of the Lutaoyang community.

Table 1
Comparison of ENVI-met and RayMan simulation tools.

Items	ENVI-met	RayMan
Model algorithm	Computational fluid dynamic based prognostic model	Diagnostic based model
Computing requirement	Computing intensive	Less computing resource required
Simulation domain	Capable of simulating the spatial distribution of thermal condition of a space.	Simulate the thermal condition only of a single point.
Modeling and calculation time	Time-consuming modeling process (Should accurately model the entire physical environments for numerical simulation.)	Quick modeling process (Capable of adopting fisheye photos in calculating thermal condition.)
Meteorological variable input	Depends on initial input climate condition for calculating next time step's environmental thermal condition.	Capable of continuously feeding in new climatic variables for assessing transient thermal condition.

living spaces. That study revealed 79.7% area of the outdoor environment exhibits high heat stress under existing environmental context, however, it further suggests that by implementing proper integrated environmental design the overheat area could be reduced to 40.5%.

2.2.2. Documenting of users' moving behavior by observation

To identify the space usage intensity and the type of space user (tourist or resident), we conducted 12 times of monthly observation in a year. Each observation was conducted on an hourly base from 8:00 to 17:00 by riding a bicycle with each cycling time from 15 min to 30 min to accomplish a cycling round. The number of space user and their distribution were paper documented together with digital camera recording for post verifying the interaction between users and the space. By this means, we can identify the people gathering hotspots and understand the density of space user in different time frames and seasons of every zones in the community.

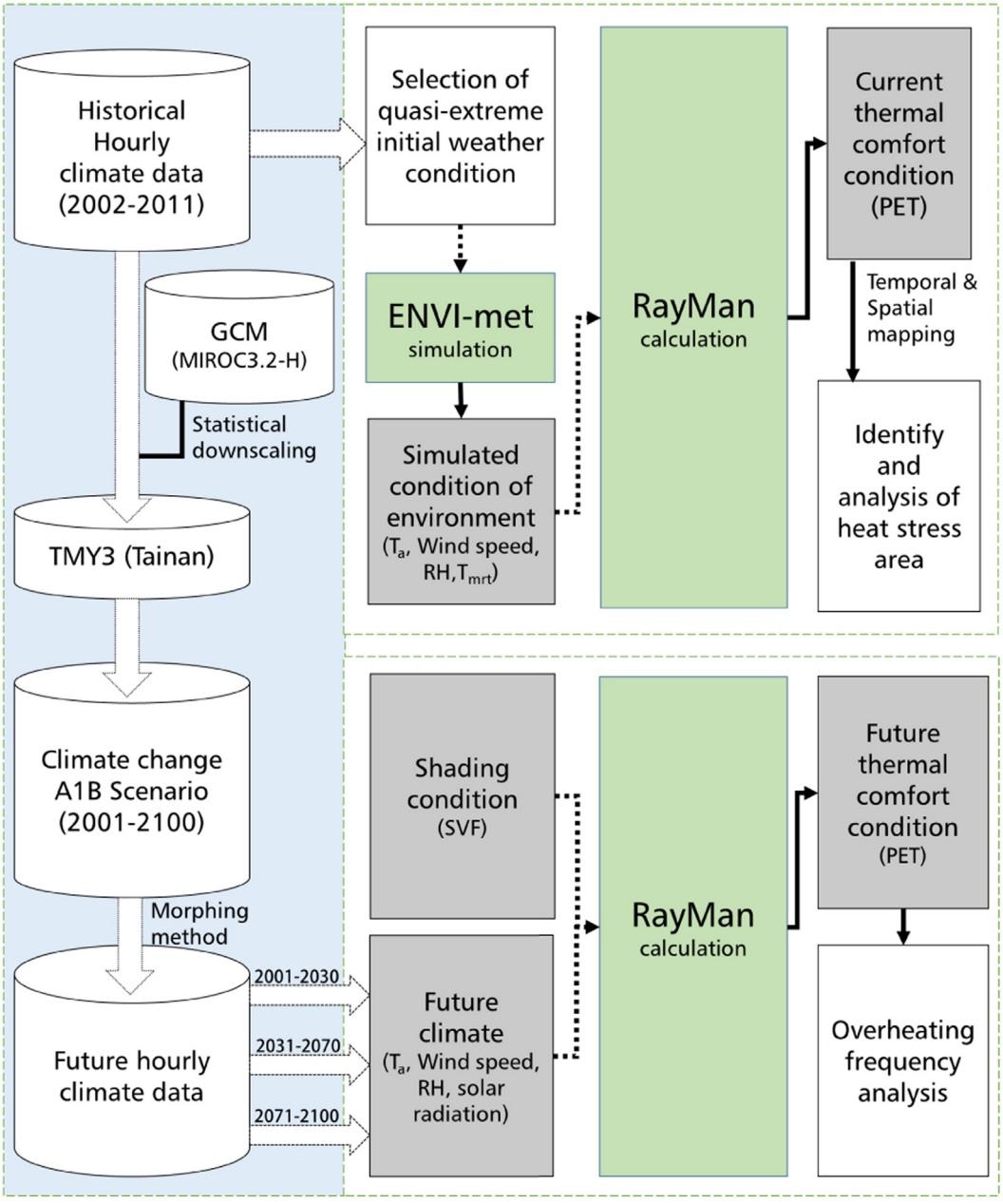

Fig. 3. The diagram of input-output dataflow and the simulation tools used for the thermal environment prediction.

2.2.3. Environmental simulation tools

Two simulation tools, ENVI-met and RayMan, were used in this research. ENVI-met is a prognostic model for simulating urban and outdoor physical environment interactions of heat, moisture and particles, including ambient potential temperature, MRT, wind velocity and its direction (Conry et al., 2015). There are a variety of applications on research using ENVI-met, including study topics on thermal adaptation strategies using vegetation (Chen and Ng, 2013; Chow and Brazel, 2012; Conry et al., 2015; Declet-Barreto et al., 2013; Fahmy et al., 2010; Frohlich and Matzarakis, 2013; Hedquist and Brazel, 2014; Hien and Jusuf, 2008; Hofman and Samson, 2014; Ketterer and Matzarakis, 2014; Ng et al., 2012; Perini and Magliocco, 2014; Skelhorn et al., 2014; Srivanit and Hokao, 2013; Wang and Akbari, 2014; Wang and Zacharias, 2015; Wania et al., 2012), pavement materials (Carnielo and Zinzi, 2013; Emmanuel and Fernand, 2007; Taleghani et al., 2014; Wang and Akbari, 2014), type of soils (Chow et al., 2011; Yang et al., 2013b). Some literatures studied the environmental differences before and after the remodeling of building layout, site planning (Berkovic et al., 2012; Taleb and Abu-Hijleh, 2013; Taleb and Taleb, 2014; Taleghani et al., 2015) or landscape design (Dutemeyer et al., 2013; Frohlich and Matzarakis, 2013; Minella et al., 2014; Perini and Magliocco, 2014; Taleb and Abu-Hijleh, 2013; Wang and Zacharias, 2015). There are also researches studying the influences of the changing climate on the future environment (Dutemeyer et al., 2013; Peng and Elwan, 2014) using ENVI-met.

As regards to RayMan, it is generally a diagnostic model and is primarily used for calculating PET within a given spatial configuration. The model itself contains building mockup interface and is able to import fisheye photos for calculating shading ratio. The customized outdoor climate data can also be imported into the model for estimating PET. Previous research using RayMan model are mostly focused on assessing the differences of outdoor thermal comfort in various microclimate conditions, such as shaded and unshaded environments, and for post analysis of thermal comfort after environmental remodeling (Balslev et al., 2015; Shiue and Matzarakis, 2011).

The comparison of both tools is given in Table 1. Due to the fact that ENVI-met is a prognostic model, which it relies on the initial inputted meteorological conditions to iteratively calculate the physical conditions of the next time step, limited capacity of dynamic weather information inputted for each calculation time step resulting simultaneously climatic calculation unviable. However, long-term weather calculation is required for studying the effect of future climate change. Therefore, we utilized the established hourly future weather datasets for calculating the future thermal environment conditions via RayMan instead. Summarily, ENVI-met is generally used for spatial distribution analysis of thermal environment in the community, and RayMan is used for analyzing the variation of future thermal conditions and the effectiveness of the proposed shading adaptation measures to counteract climate change in this study. The dataflow diagram of meteorological data processed and input to two simulation tools are depicted in Fig. 3.

2.3. Defining high thermal risk area

The determinants of risk defined in IPCC (Cardona et al., 2012; IPCC, 2014) were adopted to help identify thermal risk areas in the community by analyzing its outdoor micro-climate. The determinants of risk include three aspects: hazard, exposure, and vulnerability. Hazard signifies the possibility of adverse effects in the future (UNDRO, 1980), such as natural disaster of heavy rain or extreme climate. Exposure refers to the inventory of elements in an area in which hazard events may occur (UNISDR, 2004). Vulnerability refers to the propensity of exposed elements such as human beings, to suffer adverse effects when impacted by hazard events (UNDRO, 1980). Previous study has tried to apply these aspects to determine the risk in a certain area (Miranda Sara et al., 2016).

In this study, the corresponding layer of each aspect in the concept of risk in IPCC AR5 was constructed. The highest thermal risk area is therefore identified by observing the overlapped area from superimposing the layers of the above three aspects. Take the influence of high temperature on human body as an example, areas with the highest risk is determined by where there is high thermal stress (high hazard); where there is people constantly gathering (high exposure); and where the space users are prone to be influenced by thermal stress (high vulnerability). The definitions of the layers in hazard, exposure, and vulnerability perspectives are given below:

Fig. 4. Outdoor activity behavior of different space users observed via camera. (a) Tourists using umbrellas as thermal adaptation measures at open space; (b) tourists take shades under limited shading area; (c) common activity behavior of the residents; (d) residents adaptively modifying alley with overhead shading to resist solar radiation.

Table 2
Annual climatic statistics in the present and future time slices.

	Present (1998–2010)	Near future (2011–2040)	Midterm future (2041–2070)	Far future (2071–2100)
Daily average global solar radiation (W/m^2)	298.4	292.1	305.6	312.5
Annual average air temperature (C)	25.6	26.9	27.8	28.8

2.3.1. Layer of hazard (extreme thermal condition): thermal stress occurred in the space

The hazard is defined as the thermal stress occurred in the space. The PET index is used for evaluating the risk of thermal stress for a given space. Higher PET value denotes there is higher degree of encountering thermal risk. ENVI-met is used to simulate the entire thermal environment of the community. A typical high temperature summer date (1st August) is selected for simulation. A top 10 percentile air temperature (28.4 °C) at 4:00 in the morning statistically calculated from 2002 to 2011 long-term local weather observation is chosen for initial temperature input. The initial value of wind speed, also calculated from the same long-term weather observation, is 3.0 m/s with the prevailing wind direction from southwest. A total of 48 h from the beginning of 4:00 on 1st August were simulated, and the results of the second day were used for further analysis. Finally, the simulated PET spatial distribution at 14:00 is chosen to construct the community's thermal stress map.

2.3.2. Layer of exposure: the usage intensity of the space

The exposure is defined as the spatial intensity distribution of the space user. The area with greater number of people gathering denotes there is higher exposure exhibited. The number of people and the time of using the outdoor space were monitored for calculating the usage intensity of the space to construct spatial and temporal layer of exposure. The construction of exposure layer begins from zoning the

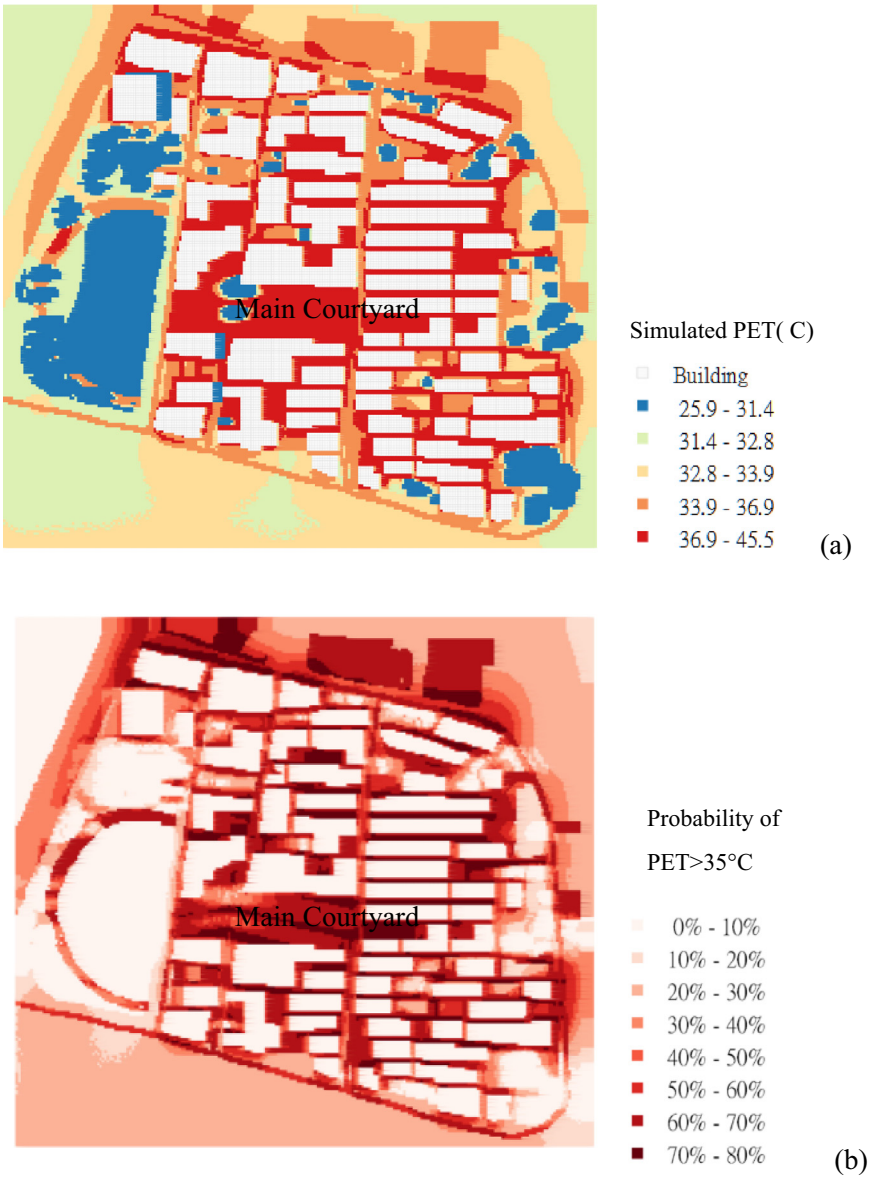

Fig. 5. Layers of spatial thermal stress. (a) Simulated PET distribution at 14:00; (b) spatial distribution of PET exceeding 35 °C.

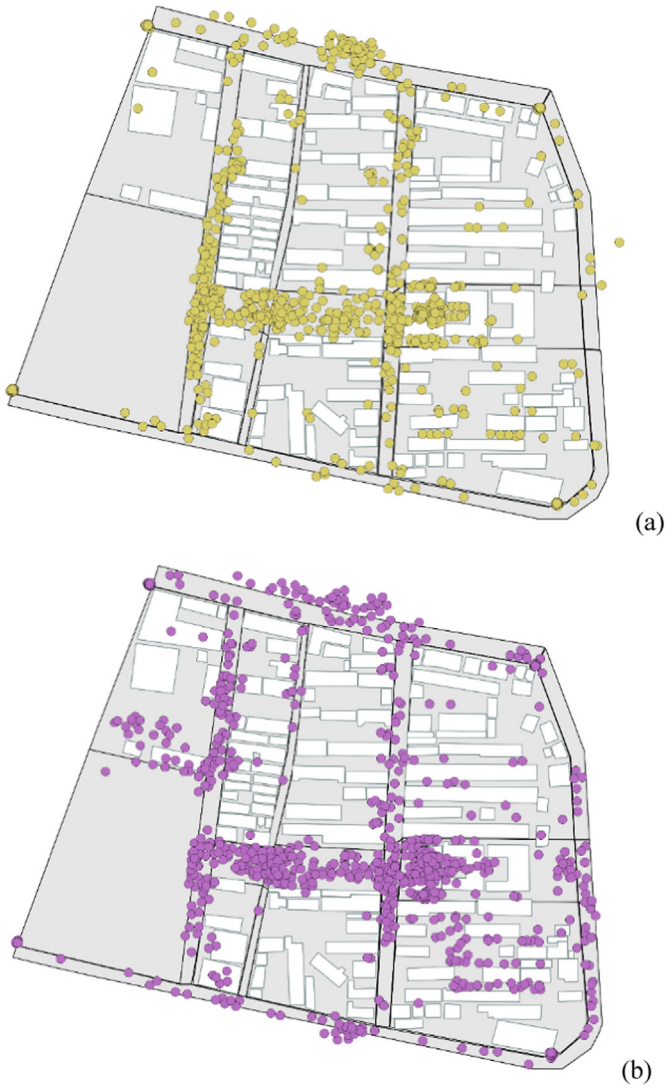

Fig. 6. Layers of the number of people distribution in outdoor space. (a) Before noon (08:00–11:00); (b) afternoon (12:00–17:00).

community's outdoor space into 22 zones based on the space's usage characteristics (touristic or residential). Secondly, the number of people within each zone is accordingly calculated. Thirdly, the usage intensity of each zone is calculated by dividing the number of people within the zone by the total number of people in the entire outdoor space of the community during the same time period.

2.3.3. Layer of vulnerability: the adaptability of the user

According to Lin and Matzarakis (Lin and Matzarakis, 2008), tourists have different perception of thermal comfort as compared to the residents, and this would result in different durability and vulnerability against thermal stress. By in-situ observation, we found that residents would usually go out in the early morning and go back to indoors at around 10:00 to 15:00 when the solar radiation is high. Afterwards, they will go out again in the late afternoon after 15:00. The residents' usage of outdoor space is quit dependent to the intensity of solar insolation. As for the tourists, they usually arrive at 11:00–14:00 when the solar radiation is high due to the inflexible itinerary schedule pre-arranged by tourism agents. The tourists can only adapt themselves to the hot climate by adjusting their clothing, using sun shading umbrellas, or resting underneath the shading objects, as depicted in Fig. 4(a) and (b).

From in-situ observation, it reveals that residents are generally much more accustomed to local environment, and have relatively abundant knowledge, experiences, or resources to adapt to the local climate, resulting lower vulnerability to thermal stress than tourists, as Fig.4(c) and (d). Therefore, the areas where the residents are constantly used are regarded as lower hazard spaces, and those used by tourists are deemed to be vulnerable spaces.

2.4. Future hourly climatological data preparation

To investigate the effect of future climate change on outdoor thermal environment of the studied building site, hourly future weather time series are required. The future hourly weather data were prepared based on the Morphing Method proposed by Belcher, which had been used in many studies (Holmes and Hacker, 2007; Robert and Kummert, 2012; Roberts, 2008; Wang et al., 2010), and had been applied successfully in Taiwan (Huang and Hwang, 2016). The morphing method adopts either shifting, linear stretching, or a combination of shifting and stretching to morph the existing observed weather variables based on the predicted meteorological changes in general circulation model (GCM) for spatial-temporal downscaling processes. The local typical meteorological year (TMY), which was constructed based on a

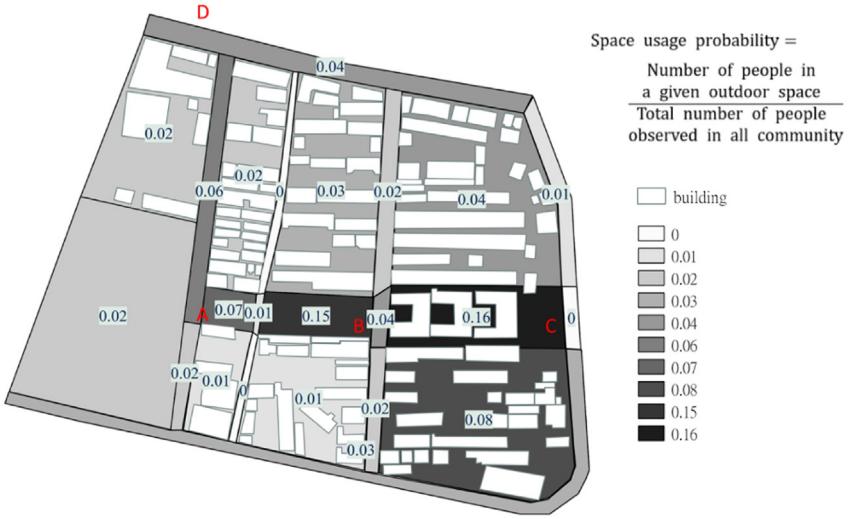

Fig. 7. Monotone layer of space usage probability (point A is entrance of the historical site; point B is the Main Courtyard; point C is the Ancestral Hall; point D is the tourists' parking lot).

Fig. 8. Space adaptability zoning based on the user charactersitcs, where "1" denotes to places with greater adaptability to thermal stress and "2" denotes to places with lower adaptability to thermal stress.

10 years' long-term hourly weather observation data from 2002 to 2011 of Tainan, was prepared as basis for morphing process. The GCM used herein is MIROC3.2-H (Japan) model. This model had been well validated against historical observed weather data nearby Taiwan (Lam et al., 2010a; Lam et al., 2010b; Lam et al., 2010c) and was considered the best-fit model for Taiwan's application among various GCMs developed based on the Fourth Assessment Report (AR4) published by IPCC (IPCC et al., 2007). Weather elements being morphed herein include atmospheric pressure, dry-bulb temperature, relative humidity, wind velocity and global horizontal solar irradiation. The readers can further explore the detail future hourly weather construction process by referring to.

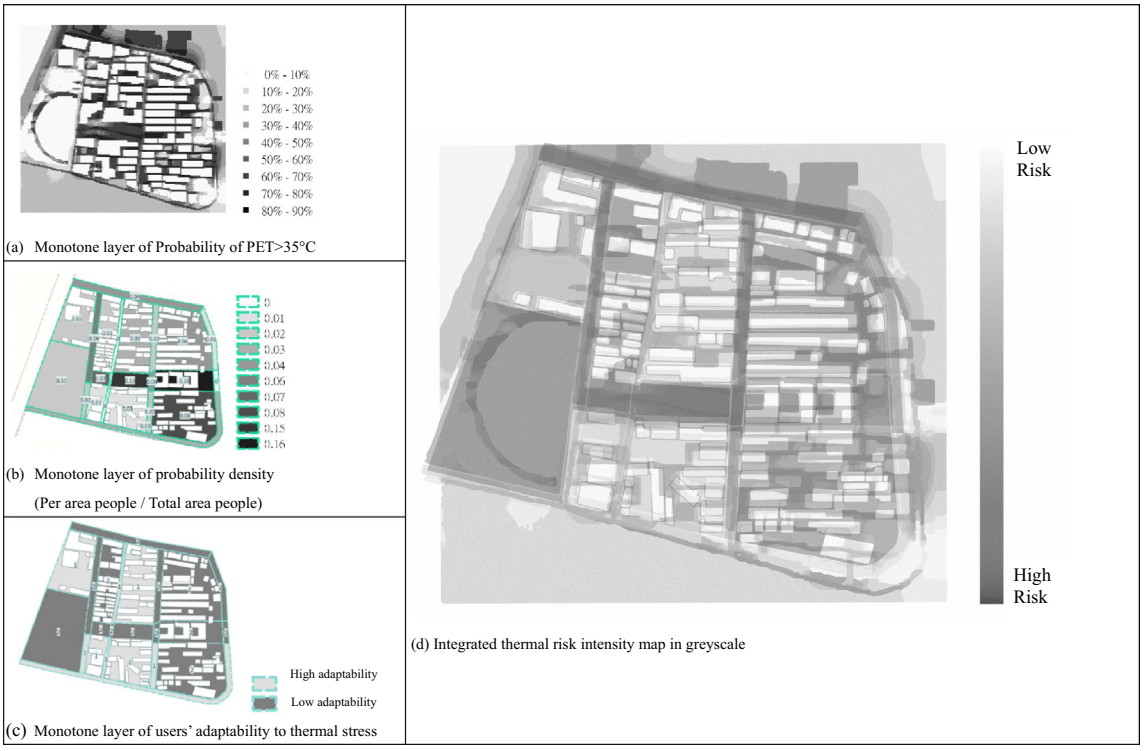

Fig. 9. The construction of micro-climate information integrated thermal risk map.

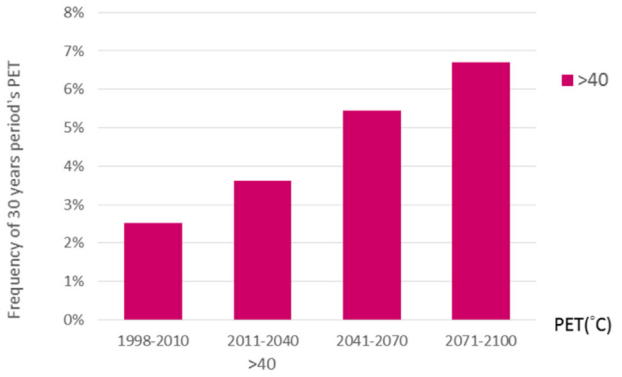

Fig. 10. Probabilities of PET exceeding 40 °C in present time against three future time slices.

The hourly future weather is established based on SRES A1B scenario (IPCC, 2000) (medium forcing with a balanced emphasis on all energy sources usage), which is deemed in accordance with the current trend of human development and activities. Three future weather time slices, 2011–2040, 2041–2070 and 2071–2100, which accordingly represent the near, mid-term, and far future were constructed. Each future time slice contains hourly weather data of 30 consecutive years and their weather statistics are tabulated in Table 2.

2.5. Definition of thermal comfort range

There are variety of indicators that integrate thermal environmental factors with human heat balance for assessing the thermal comfort condition of outdoor spaces. PET has been adopted in the German VDI 3787 (VDI, 1998), and has been widely used in various outdoor thermal comfort researches. It is a thermal comfort index, which is defined as the outdoor complex environment, for the heat balance of the human body; in a typical indoor setting (where the ambient temperature equals MRT, vapor pressure = 12 hPa, wind velocity = 0.1 m/s), the heat budget of the human body is balanced to the same core and skin temperature as those under complex outdoor conditions. Thus, PET enables people to compare the outside integral effects of complex thermal conditions with their experience indoors (Höppe, 1999; Mayer and Höppe, 1987). As PET fully considers the impact of outdoor shortwave and longwave radiation properties of body heat balance, it is suitable for outdoor thermal comfort assessment. Therefore, this study used PET as a representative of thermal stress indicators, and are calculated by the RayMan model (Matzarakis et al., 2007a; Matzarakis et al., 2007b; Matzarakis et al., 2010).

The classification of the perceived temperature of Taiwan is referenced from (Lin and Matzarakis, 2008) and is adopted herein for thermal comfort assessment. As proposed by (Lin and Matzarakis, 2008) the PET range is classified into seven thermal perception categories, where PET < 16 °C is cold, 16–20 °C is cool, 21–25 °C is slightly cool, 26–31 °C is comfort, 32–36 °C is slightly warm, 37–40 °C is warm, and PET > 40 °C is considered hot. In this study, for areas with PET > 40 °C is deemed as areas encountering thermal stress and is thermally unacceptable.

3. Results

3.1. Identify the focused risk area

According to the method described in Section 2.3, three layers including thermal stress, space usage intensity, and the vulnerability of users were constructed. By superimposing these three layers, various degrees of outdoor thermal risk of the community can be visually distinguished.

3.1.1. Spatial distribution of thermal stress

The risk determinant "hazard" is interpreted as environmental thermal stress in this study. Higher thermal stress means that the user's body is more prone to be influenced by heat resulting uncomfortable feelings. Fig. 5(a) clearly demonstrates the spatial distribution of simulated PET at 14:00 on the typical summer day. It is found that the PET is

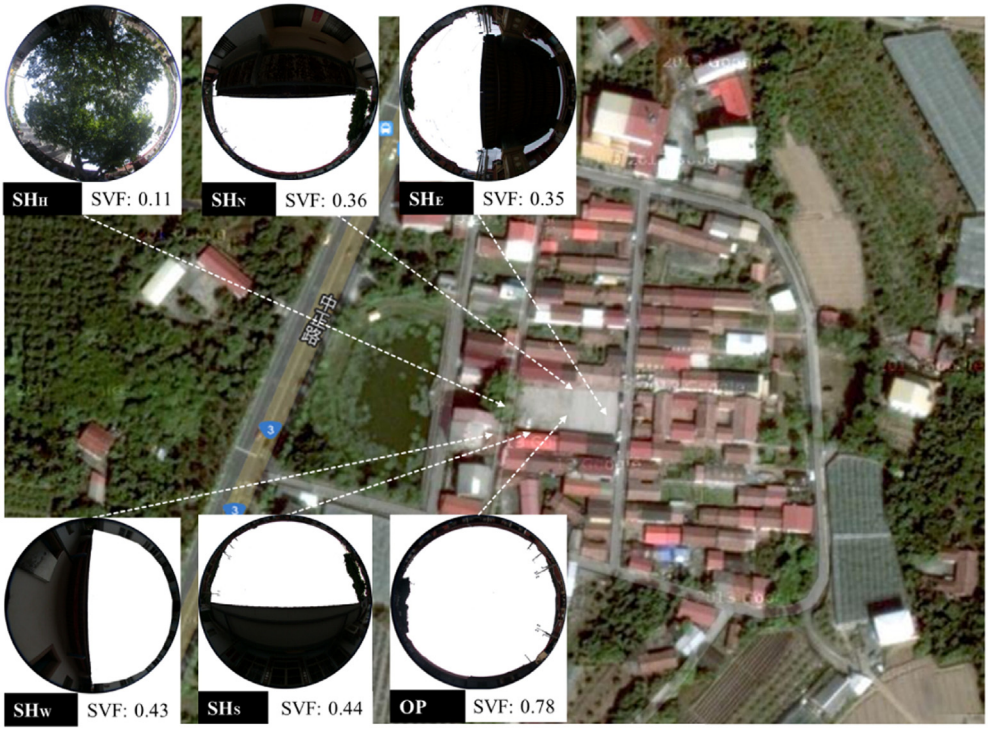

Fig. 11. Shading characteristics in the focused risk area. (SH_H denotes to highly shaded area; SH_S denotes to shading at the south side; SH_E is shading at the east side; SHW is shading at the west side and OP denotes to open space which is at the center of the courtyard.)

higher between buildings, on the asphalt-paved roads, and at the open space where there is no shading, particularly at the Main Courtyard of the community. Fig. 5(a) only reveals the thermal environment distribution at a certain time (14:00). However, in order to discuss the diurnal temporal distribution of thermal stress, we further retrieved hourly PETs from 08:00 to 18:00 of each simulated grid and calculated the probability of PET being larger than 35 °C, as illustrated in Fig. 5(b). It reveals that there is only 20% probability of PET exceeding 35 °C for places with shading. In contrast, there is around 50% probability for open space areas without shading. We observed that the unshaded Main Courtyard would exhibit higher PET than the other places for the reason that it receives considerable amount of direct solar irradiation.

3.1.2. Spatial distribution of usage intensity

The risk determinant "exposure" is interpreted as usage intensity of space in this study. High space usage intensity denotes there is higher probability that the user will expose to thermal stress in perspective of the number of people and their total exposure time. Fig. 6(a) and (b) shows the spatial distribution of the number of user before noon (08:00–11:00) and after noon (12:00–18:00) respectively during summer diurnal period. Although the distribution of the number of user is similar, people are more concentrated between roads from Main Courtyard (point B) to Ancestral Hall (point C) in the afternoon, as depicted in Fig. 6(b). The space usage intensity in the vicinity of Main Courtyard in the afternoon is greater than that in the morning.

The method used for area zoning to present the calculated space usage intensity follows the description in Section 2.3.2. From the usage intensity distribution shown in Fig. 7, the highest usage intensity area (42%) is along the spatial axis from point A to C, follows by the road areas and the southeast part of the community. We found that the space usage intensity will vary with visiting paths where the environment is beautified with horticultural gardens or featured pavements.

3.1.3. Spatial distribution of users' vulnerability

The risk determinant "vulnerability" is interpreted as spatial distribution of users' adaptability capacity in this study. The spaces typically used by the residents are regarded as places with lower vulnerability, as zones marked with "1" in Fig. 8. Whereas the spaces typically used by tourists are regarded places with higher vulnerability and are marked as "2". The tourists' path usually begins from point D (parking area) walking alongside the major road to point A (the entrance) and to the major visiting point B (the Main Courtyard) and C (Ancestral Hall). It reveals that the planning of the visiting routes will affect the moving pattern of the tourists and it also demonstrates that the

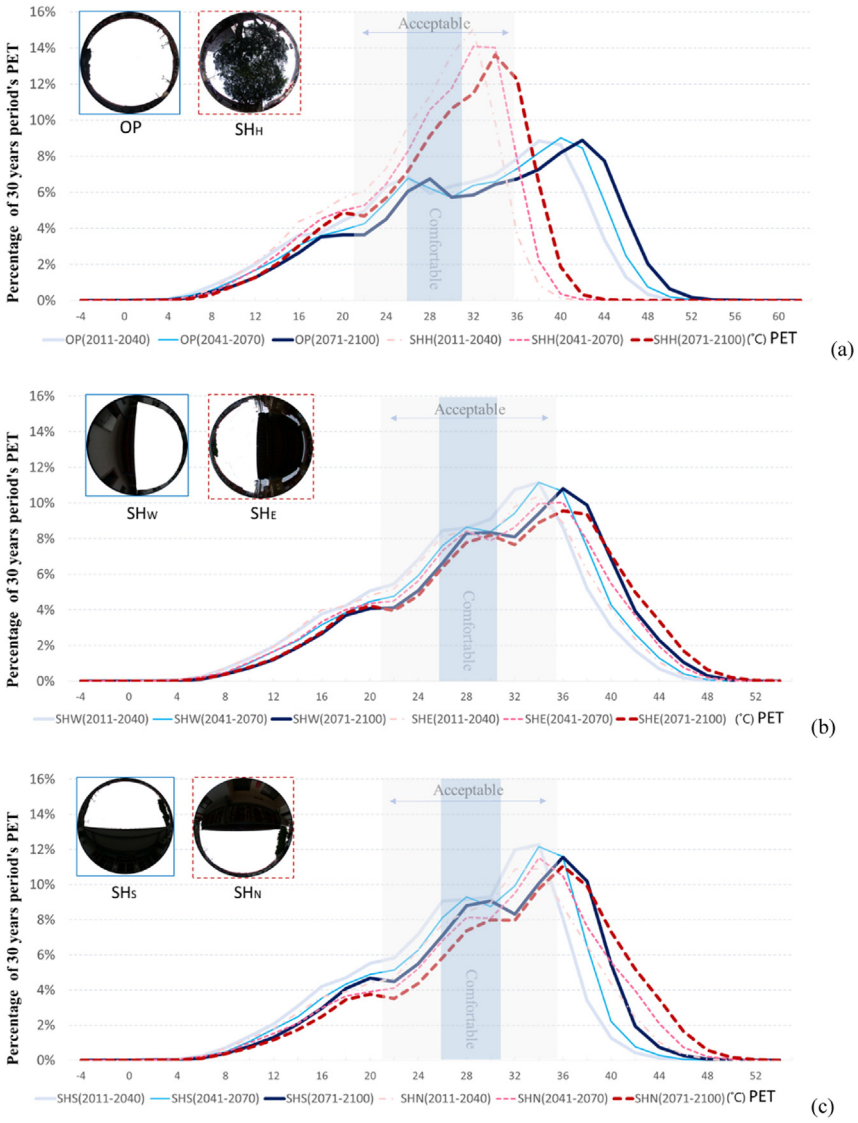

Fig. 12. Pattern variations of PET frequency distribution of various shading characteristcs in three future time slices. (a) open space (OH) against highly shaded space (SH_H); (b) shading at west side (SH_W) against shading at east side (SH_E); (c) shading at south side (SH_S) against shading at north side (SH_N).

geographical planning of visiting routes and functional spaces will greatly determine the spatial distribution of the users.

3.1.4. Identifying the focused risk area

As described in Section 2.3, the layers of thermal stress distribution, space usage intensity distribution, and the spatial distribution of users' vulnerability are superimposed based on the brightness level of monotone greyscale from each layer map as demonstrated in Fig. 9. The areas with brighter greyscale represent lower risk, and those with darker greyscale means it will exhibit higher thermal risk potentially. From Fig. 9, the darkest greyscale shown at the Main Courtyard reveals that this location has the highest thermal risk and is deemed as the focused risk area where is worth further analyzed and discussed with.

3.2. Thermal comfort trend from the analysis of the constructed future climate data

To have a general glimpse on the future variation trend of thermal comfort, we tried to calculate hourly PET solely based on the future weather data constructed based on method described in Section 2.4 regardless of physical environment. By this mean, the calculated PET is analogous to the results derived from an unshaded open space environment. The calculated probability of future PET exceeding 40 °C in the near, mid-term, and far future is shown in Fig. 10. As time proceeds, the probability of high temperature occurrence is increasing. The probability of PET exceeding 40 °C will be escalated by an increment of 1.1%, 2.9%, 4.2% respectively for the near, mid-term and far future as compared to nowadays.

Table 3
Variation trend of PET in three future time slices. (The values shown in the mid-term and the far future column are the relative increments as compared to their corresponding near future; and the overlaying grey color is indicative in length of the increment amount.)

Time:06-18 >95%	Hot season 3-11			Cold season 12-2		
	Near Future	Midterm	Far future	Near Future	Midterm	Far future
Base period	2011-2040	2041-2070	2071-2100	2011-2040	2041-2070	2071-2100
SHh	34.2	+ 1.3 (35.5)	+ 3.1 (37.3)	27.1	+ 1.5 (28.6)	+ 2.4 (29.5)
OP	42.4	+ 1.3 (43.7)	+ 3.0 (45.4)	34.5	+ 2.0 (36.5)	+ 3.2 (37.7)
SHn	39.9	+ 1.5 (41.4)	+ 3.0 (42.9)	33.6	+ 2.0 (35.6)	+ 3.2 (36.8)
SHs	36.5	+ 1.2 (37.7)	+ 3.0 (39.5)	28.0	+ 1.3 (29.3)	+ 2.3 (30.3)
SHe	39.9	+ 1.4 (41.3)	+ 3.1 (43.0)	31.8	+ 1.9 (33.7)	+ 3.1 (34.9)
SHw	38.9	+ 1.3 (40.2)	+ 2.8 (41.7)	30.6	+ 1.7 (32.3)	+ 2.9 (33.5)
PET legend(°C)	20	25	30	35	40	45

3.3. Future thermal comfort conditions concerning different shading orientation

Outdoor shading is a crucial factor to decrease MRT by blocking the direct solar radiation. We choose the identified focused thermal risk area, the Main Courtyard, to investigate the future thermal comfort conditions concerning different levels and orientations of shading. The level of shading is characterized as sky view factor (SVF) herein. SVF denotes the ratio between radiation received by a planar surface and that from the entire hemispheric radiating environment and is calculated as the fraction of sky visible when viewed from the ground up (Watson and Johnson, 1987). Low SVF means there is high proportion of sky obstructed by tree canopies as well as neighboring buildings and is expected to provide lower MRT. Moreover, different relative positions of tree to the user, albeit with the same SVF, will provide different degrees of cooling effect by virtue of the varying diurnal sun path. Therefore, thermal environmental differences of various SVFs and different orientations of shading with the same SVF were investigated.

Locations with highly shaded (SH_H, SVF = 0.11) area under tree's canopy and the open space (OP, SVF = 0.78) at the center of the Main Courtyard were chosen for thermal comfort study. Furthermore, places near the four sides of the Main Courtyard with their SVFs being around 0.4 were also investigated for study the shading position differences. The locations we choose for analysis is shown in Fig. 11, the subscript denotes the relative position where the shading is to the user, such as SH_E denotes shading at the user's east side. The hourly PETs distributions for each future time slices are calculated by importing the corresponding SVF fisheye photos and the future climate data into RayMan model. By this, the long-term shading effectiveness under the influence from future climate can be analyzed.

3.3.1. Annual variation trend

The hourly thermal comfort conditions in the future due to climate change is simulated via RayMan and is presented as PET index. For each location with different shading characteristics, the annual occurrence probability of PET in the three future time slices was illustrated in Fig. 12. The overheating occurrence frequency (F_{oh}) index is used for describing the thermal environmental change in the context of climate change. The F_{oh} is defined as a fraction of the hours when PET exceeds 40 °C divided by the total diurnal hours. Higher F_{oh} denotes higher potential of thermal risk.

From Fig. 12, we observed that the occurrence of high PET increases as time proceeds for all shading cases, which is believed a result from higher ambient temperature in the future. The F_{oh} is 12.5% higher in the far future (2071–2100) as compared to that of the near future (2011–2040) for unshaded open space (OH) case. On the contrary, it will only increase by 2.1% for the highly shaded (SH_H) area for the same period. The areas with limited shading will exhibit much higher thermal risk than those with shades, which confirms the effectiveness of shading as outdoor countermeasure to climate change.

The F_{oh} of SH_N is higher than that of SH_S because of the limited capacity of direct solar radiation obstruction for the shading located at the north side. Moreover, the F_{oh} of SH_N is 6.4% and 10.0% higher than that of SH_S in near and far future time slices respectively. It demonstrates that as time proceeds the thermal comfort will worsen for places where the shading is primitively limited. As depicted in Fig. 12(c), the F_{oh} of SH_E is higher than SH_W because of the higher temperature and the limited sun blocking capacity for SH_E case in the afternoon. The F_{oh} of SH_E is higher than SH_W by 2.2% and 3.6% in the near and far future respectively, revealing that thermal comfort at SH_E will be worsening over time. In general, shading at south (SH_S) provides better thermal environment than the others, follows by SH_W, SH_E, and SH_N. A significant trend is observed that the increment of thermal discomfort in the future will be amplified as time proceeds for places with less shading.

3.3.2. Seasonal variation trend

We further characterized the seasonal variation trend of the six locations by calculating the temperature at the top 5 percentile of the cumulative distribution of diurnal PET (06:00 to 18:00) during the warm season (March to November) and the cool season (December to February) for each future time slices. The results are tabulated in Table 3. The PET is 8.2 °C and 7.4 °C lower at SH_H as compared to OP location in warm and cool season respectively in the near future which proves the capacity of shading for thermal stress mitigation. By further observing the increments in the mid-term and the far future time slices, although the amounts of the increment are similar for both SH_H and OP area in warm season, it is +1.5 °C and +2.4 °C for SH_H as compared to +2.0 °C and +3.2 °C for OP in cool season. The amplitude is expanding obviously over time in cool season, revealing shading strategy is more effective in alleviating the climate change impact to thermal stress in cool season than in warm season. Similar trend is observed for cases with different shading position. In summary, for those cases with more thermal stress at present time, may be vastly aggravated under the influence of future climate change.

3.3.3. Diurnal variation trend

The number of space user, as depicted in Fig. 6, is diverse in the morning and in the afternoon. Therefore, the future thermal environment variation before and after noon is further discussed. The frequencies of PET exceeding 40 °C (F_{oh}) before and after noon for locations with different shading position is shown in Fig. 13. It is obvious that higher discomfort probability is observed at SH_W before noon and at SH_E in the afternoon, where the relative positions of shading at both locations are unable to effectively block the solar radiation due to the sun's position at that time. However, the thermal comfort condition at

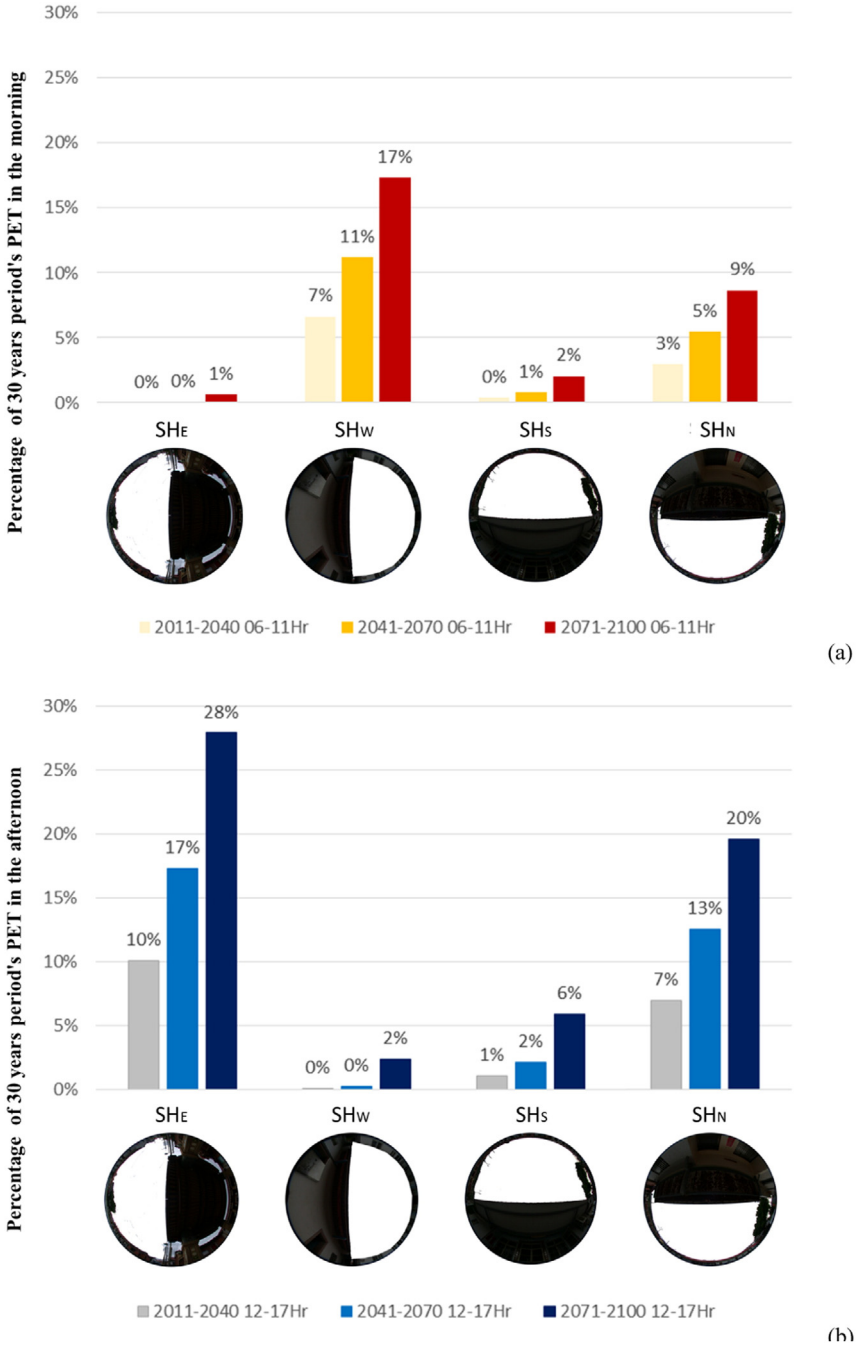

Fig. 13. Occurrence frequencies of PET exceeding 40 °C at various shading locations. (a) Before noon (06–11 Hr); (b) After noon (12–17 Hr).

SH_E in the afternoon have more significant deterioration than that at SH_W in the morning as time proceeds towards future, signifying that SH_E is more vulnerable to the changing climate than SH_W. Shading improvement is much more demanded for location at SH_E.

The analysis results reveal that different degrees of thermal stress will occur in different periods of time during a day, and is dependent to the relative position of the shading. Accordingly, the space usage behavior, including whom and when is using the space, should be considered when scheming up countermeasures to improve thermal environment. Tourists, who usually are less adaptive to local thermal stress than the residents and are often have visiting activities in the afternoon, should be of prior concern. Therefore, the first priority location needed to be thermally improved in the community is at SH_E, where it is a tourists' hot spot with limited shading in the afternoon.

4. Conclusions

In this study, we proposed a novel approach to appraise environmental thermal stress of a traditional community based on thermal risk identification. To identify focused risk areas, we followed and reinterpreted the concepts of hazard, exposure, and vulnerability defined by IPCC. This approach is different from the traditional assessment method, which only uses single index for identifying thermal risk area, such as temperature. The method integrates various aspects of information related to the targeted issue to help facilitate analysis. However, it's crucial to clearly define the "risk" in advance for implementing this method. This research applied the concept of thermal risk assessment, using data derived from both in-situ measurement as well as simulation results to construct spatial distribution layers of thermal stress, space usage intensity, and user's vulnerability of the community. The focused risk area is identified by mapping the above layers for evaluating the existing environmental conditions of that area against the changing climate. Furthermore, we integrated both prognostic and diagnostic simulation models for predicting the thermal environment. Prognostic model, ENVI-met, is used for simulating the outdoor thermal stress distribution of the community on short-term basis, and the diagnostic model, RayMan, is used for predicting the long-term future thermal conditions due to climate change.

Once the thermal risk area has been identified, thermal stress countermeasures to climate change specifically to that area can subsequently be formulated based on the aspects of hazard, exposure and vulnerability. The advantage of this thermal environment diagnostic solution approach is that it's quite straightforward in reaching objective adaptation solutions. However, the limitation is that with the diverse adaptation methods and responses derived from this approach, it relies knowledge from the local experiences or experts' insights to reach practical solutions for implementation. Nevertheless, following conclusions were reached:

1. To evaluate the influence of future climate on thermal stress, a morphing approach was applied to produce future hourly weather data based on GCMs in three future time slices. The constructed future weather reveals a significant trend of temperature and solar radiation rising, which suggests the thermal environment will be deteriorated as time proceeds. The probability of PET exceeding 40 °C will be escalated by an increment of 1.1%, 2.9%, 4.2% respectively for the near, mid-term and far future as compared to nowadays, which corresponds to an increment rate of 44%, 116%, 168%. It suggests high PET will be occurred more frequently in the future, resulting higher probability of encountering thermal stress for outdoor activities during warm seasons.
2. To promptly assess thermal environment conditions in the present and future time and with the constraint of the limited computing capacity for prognostic simulation with enormous future climate data, the prognostic and diagnostic outdoor thermal environment simulation models were jointly used and is found feasible in this research.
3. The adaptation strategies of outdoor shading in response to climate change were proposed based on the synthesis reasoning from the temporal and spatial distributions of the users, the outdoor thermal stress, and the users' vulnerability. The focused thermal risk area is identified and is located at the Main Courtyard where there is limited shading and has relatively large number of people gathering. We found that the east side of the courtyard (SH_E) with the building shades at the east, exhibited the highest risk of thermal stress in facing climate change, due to the reason that thermal environment in the afternoon would deteriorate more than that in the morning hours.

From the above results, we recommend the outdoor environmental assessment which needs to consider the local building context related to thermal environment. Furthermore, human behavior is important for the identification of the thermal risk evaluation. Based on this information, the suitable adaptions may further developed based on the issue of climate change.

Acknowledgments

The authors would like to thank the Ministry of Science and Technology of Taiwan, for financially supporting this research under Contract No. 102-2221-E-006-292-MY2 and 104-2221-E-006-217-MY3.

References

Balslev, Y.J., Potchter, O., Matzarakis, A., 2015. Climatic and thermal comfort analysis of the Tel-Aviv Geddes Plan: a historical perspective. Build. Environ. 93, 302–318.
Berkovic, S., Yezioro, A., Bitan, A., 2012. Study of thermal comfort in courtyards in a hot arid climate. Sol. Energy 86, 1173–1186.
Brosy, C., Zaninovic, K., Matzarakis, A., 2014. Quantification of climate tourism potential of Croatia based on measured data and regional modeling. Int. J. Biometeorol. 58, 1369–1381.
Cardona, O.D., van Aalst, M.K., Birkmann, J., Fordham, M., McGregor, G., Perez, R., et al., 2012. Determinants of risk: exposure and vulnerability. A Special Report of Working Groups I and II of the Intergovernmental Panel on Climate Change (IPCC). Managing the Risks of Extreme Events and Disasters to Advance Climate Change Adaptation. Cambridge University Press, Cambridge, UK, and New York, NY, USA, pp. 65–108.
Carnielo, E., Zinzi, M., 2013. Optical and thermal characterisation of cool asphalts to mitigate urban temperatures and building cooling demand. Build. Environ. 60, 56–65.
Chen, L., Ng, E., 2011. Quantitative urban climate mapping based on a geographical database: a simulation approach using Hong Kong as a case study. Int. J. Appl. Earth Obs. Geoinf. 13, 586–594.
Chen, L., Ng, E., 2013. Simulation of the effect of downtown greenery on thermal comfort in subtropical climate using PET index: a case study in Hong Kong. Archit. Sci. Rev. 56, 297–305.
Cheung, C.S.C., Hart, M.A., 2014. Climate change and thermal comfort in Hong Kong. Int. J. Biometeorol. 58, 137–148.
Chow, W.T.L., Brazel, A.J., 2012. Assessing xeriscaping as a sustainable heat island mitigation approach for a desert city. Build. Environ. 47, 170–181.
Chow, W.T.L., Pope, R.L., Martin, C.A., Brazel, A.J., 2011. Observing and modeling the nocturnal park cool island of an arid city: horizontal and vertical impacts. Theor. Appl. Climatol. 103, 197–211.
Conry, P., Sharma, A., Potosnak, M.J., Leo, L.S., Bensman, E., Hellmann, J.J., et al., 2015. Chicago's heat island and climate change: bridging the scales via dynamical downscaling. J. Appl. Meteorol. Climatol. 54, 1430–1448.
Csete, M., Palvolgyi, T., Szendro, G., 2013. Assessment of climate change vulnerability of tourism in Hungary. Reg. Environ. Chang. 13, 1043–1057.
Declet-Barreto, J., Brazel, A.J., Martin, C.A., Chow, W.T.L., Harlan, S.L., 2013. Creating the park cool island in an inner-city neighborhood: heat mitigation strategy for Phoenix, AZ. Urban Ecosyst. 16, 617–635.
Dutemeyer, D., Barlag, A.B., Kuttler, W., Axt-Kittner, U., 2013. Measures against heat stress in the city of Gelsenkirchen, Germany. Erde 144, 181–201.
Emmanuel, R., Fernand, H.J.S., 2007. Urban heat islands in humid and arid climates: role of urban form and thermal properties in Colombo, Sri Lanka and Phoenix, USA. Clim. Res. 34, 241–251.
Fahmy, M., Sharples, S., Yahiya, M., 2010. LAI based trees selection for mid latitude urban developments: a microclimatic study in Cairo, Egypt. Build. Environ. 45, 345–357.
Frohlich, D., Matzarakis, A., 2013. Modeling of changes in thermal bioclimate: examples based on urban spaces in Freiburg, Germany. Theor. Appl. Climatol. 111, 547–558.
Gromke, C., Blocken, B., Janssen, W., Merema, B., van Hooff, T., Timmermans, H., 2015. CFD analysis of transpirational cooling by vegetation: case study for specific meteorological conditions during a heat wave in Arnhem, Netherlands. Build. Environ. 83, 11–26.
Hedquist, B.C., Brazel, A.J., 2014. Seasonal variability of temperatures and outdoor human comfort in Phoenix, Arizona, USA. Build. Environ. 72, 377–388.
Hien, W.N., Jusuf, S.K., 2008. GIS-based greenery evaluation on campus master plan. Landsc. Urban Plan. 84, 166–182.

Hofman, J., Samson, R., 2014. Biomagnetic monitoring as a validation tool for local air quality models: a case study for an urban street canyon. Environ. Int. 70, 50–61.
Holmes, M.J., Hacker, J.N., 2007. Climate change, thermal comfort and energy: meeting the design challenges of the 21st century. Energ. Build. 39, 802–814.
Höppe, P., 1999. The physiological equivalent temperature – a universal index for the biometeorological assessment of the thermal environment. Int. J. Biometeorol. 43, 71–75.
Huang, K.-T., Hwang, R.-L., 2016. Future trends of residential building cooling energy and passive adaptation measures to counteract climate change: the case of Taiwan. Appl. Energy 184, 1230–1240.
Huang, K.T., Lin, T.P., Lien, H.C., 2015. Investigating thermal comfort and user behaviors in outdoor spaces: a seasonal and spatial perspective. Adv. Meteorol. 2015.
Hwang, R.L., Lin, T.P., 2007. Thermal comfort requirements for occupants of semi-outdoor and outdoor environments in hot-humid regions. Archit. Sci. Rev. 50, 357–364.
Hwang, R.L., Lin, C.Y., Huang, K.T., 2017. Spatial and temporal analysis of urban heat island and global warming on residential thermal comfort and cooling energy in Taiwan. Energ. Build. 152, 804–812.
IPCC, 2000. IPCC special report on emissions scenarios. Intergovernmental Panel on Climate Change.
IPCC, 2014. Climate change 2014: impacts, adaptation, and vulnerability. Part A: global and sectoral aspects. Contribution of Working Group II to the Fifth Assessment Report of the Intergovernmental Panel on Climate Change. Cambridge University Press, Cambridge, United Kingdom and New York, NY, USA, p. 1132.
IPCC, Solomon, S., Qin, D., Manning, M., Chen, Z., Marquis, M., et al., 2007. Climate change. Contribution of the Working Group I to the Fourth Assessment Report of the Intergovernmental Panel on Climate Change., Cambridge.
Kantor, N., Unger, J., 2010. Benefits and opportunities of adopting GIS in thermal comfort studies in resting places: an urban park as an example. Landsc. Urban Plan. 98, 36–46.
Ketterer, C., Matzarakis, A., 2014. Human-biometeorological assessment of heat stress reduction by replanning measures in Stuttgart, Germany. Landsc. Urban Plan. 122, 78–88.
Kruger, E., Minella, F.O., Matzarakis, A., 2014. Comparison of different methods of estimating the mean radiant temperature in outdoor thermal comfort studies. Int. J. Biometeorol. 58, 1727–1737.
Kuwae, M., Yoshikawa, S., Tsugeki, N., Inouchi, Y., 2004. Reconstruction of a climate record for the past 140 kyr based on diatom valve flux data from Lake Biwa, Japan. J. Paleolimnol. 32, 19–39.
Lam, J.C., Wan, K.K.W., Lam, T.N.T., Wong, S.L., 2010a. An analysis of future building energy use in subtropical Hong Kong. Energy 35, 1482–1490.
Lam, J.C., Wan, K.K.W., Wong, S.L., Lam, T.N.T., 2010b. Long-term trends of heat stress and energy use implications in subtropical climates. Appl. Energy 87, 608–612.
Lam, T.N.T., Wan, K.K.W., Wong, S.L., Lam, J.C., 2010c. Impact of climate change on commercial sector air conditioning energy consumption in subtropical Hong Kong. Appl. Energy 87, 2321–2327.
Lau, K.K.L., Lindberg, F., Rayner, D., Thorsson, S., 2015. The effect of urban geometry on mean radiant temperature under future climate change: a study of three European cities. Int. J. Biometeorol. 59, 799–814.
Lee, H., Mayer, H., Schindler, D., 2014. Importance of 3-D radiant flux densities for outdoor human thermal comfort on clear-sky summer days in Freiburg, Southwest Germany. Meteorol. Z. 23, 315–330.
Lin, T.P., 2009. Thermal perception, adaptation and attendance in a public square in hot and humid regions. Build. Environ. 44, 2017–2026.
Lin, T.P., Matzarakis, A., 2008. Tourism climate and thermal comfort in Sun Moon Lake, Taiwan. Int. J. Biometeorol. 52, 281–290.
Lin, T.P., Matzarakis, A., Hwang, R.L., 2010. Shading effect on long-term outdoor thermal comfort. Build. Environ. 45, 213–221.
Lin, C.H., Lin, T.P., Hwang, R.L., 2013a. Thermal comfort for urban parks in subtropics: understanding visitor's perceptions, behavior and attendance. Adv. Meteorol. 2013.
Lin, T.P., Tsai, K.T., Liao, C.C., Huang, Y.C., 2013b. Effects of thermal comfort and adaptation on park attendance regarding different shading levels and activity types. Build. Environ. 59, 599–611.
Lin, C.-Y., Chua, Y.-J., Sheng, Y.-F., Hsu, H.-H., Cheng, C.-T., Lin, Y.-Y., 2015. Altitudinal and latitudinal dependence of future warming in Taiwan simulated by WRF nested with ECHAM5/MPIOM. Int. J. Climatol. 35, 1800–1809.
Lin, C.Y., Chien, Y.Y., Su, C.J., Kueh, M.T., Lung, S.C., 2017. Climate variability of heat wave and projection of warming scenario in Taiwan. Clim. Chang. 1–16.
Loughnan, M., Carroll, M., Tapper, N.J., 2015. The relationship between housing and heat wave resilience in older people. Int. J. Biometeorol. 59, 1291–1298.
Matzarakis, A., Endler, C., 2010. Climate change and thermal bioclimate in cities: impacts and options for adaptation in Freiburg, Germany. Int. J. Biometeorol. 54, 479–483.
Matzarakis, A., Rutz, F., Mayer, H., 2007a. Modelling radiation fluxes in simple and complex environments - application of the RayMan model. Int. J. Biometeorol. 51, 323–334.
Matzarakis, A., Rutz, F., Mayer, H., 2007b. Modelling radiation fluxes in simple and complex environments - application of the RayMan model. Int. J. Biometeorol. 51, 323–334.
Matzarakis, A., Rutz, F., Mayer, H., 2010. Modelling radiation fluxes in simple and complex environments: basics of the RayMan model. Int. J. Biometeorol. 54, 131–139.
Mayer, H., Höppe, P., 1987. Thermal comfort of man in different urban environments. Theor. Appl. Climatol. 38, 43–49.
Minella, F.O., Kruger, E., Honjo, S., Goyette, S., Hedjazi, A., 2014. Daytime microclimatic impacts of the SOVALP project in summer: a case study in Geneva, Switzerland. Simulation 90, 857–873.
Miranda Sara, L., Jameson, S., Pfeffer, K., Baud, I., 2016. Risk perception: the social construction of spatial knowledge around climate change-related scenarios in Lima. Habitat Int. 54, 136–149.
Moreno, A., Becken, S., 2009. A climate change vulnerability assessment methodology for coastal tourism. J. Sustain. Tour. 17, 473–488.
Muthers, S., Matzarakis, A., Koch, E., 2010. Climate change and mortality in Vienna-a human biometeorological analysis based on regional climate modeling. Int. J. Environ. Res. Public Health 7, 2965–2977.
Ng, E., Chen, L., Wang, Y.N., Yuan, C., 2012. A study on the cooling effects of greening in a high-density city: an experience from Hong Kong. Build. Environ. 47, 256–271.
Nikolopoulou, M., Lykoudis, S., 2007. Use of outdoor spaces and microclimate in a Mediterranean urban area. Build. Environ. 42, 3691–3707.
Noro, M., Busato, F., Lazzarin, R.M., 2015. Urban heat island in Padua, Italy: experimental and theoretical analysis. Indoor and Built Environ. 24, 514–533.
Norton, B.A., Coutts, A.M., Livesley, S.J., Harris, R.J., Hunter, A.M., Williams, N.S.G., 2015. Planning for cooler cities: a framework to prioritise green infrastructure to mitigate high temperatures in urban landscapes. Landsc. Urban Plan. 134, 127–138.
Peng, C.Z., Elwan, A., 2014. An outdoor-indoor coupled simulation framework for Climate Change-conscious Urban Neighborhood Design. Simulation 90, 874–891.
Perini, K., Magliocco, A., 2014. Effects of vegetation, urban density, building height, and atmospheric conditions on local temperatures and thermal comfort. Urban For. Urban Green. 13, 495–506.
Ren, C., Spit, T., Lenzholzer, S., Yim, H.L.S., Heusinkveld, B., van Hove, B., et al., 2012. Urban climate map system for Dutch spatial planning. Int. J. Appl. Earth Obs. Geoinf. 18, 207–221.
Robert, A., Kummert, M., 2012. Designing net-zero energy buildings for the future climate, not for the past. Build. Environ. 55, 150–158.
Roberts, S., 2008. Effects of climate change on the built environment. Energ Policy 36, 4552–4557.
Scott, D., Steiger, R., Rutty, M., Johnson, P., 2015. The future of the Olympic Winter Games in an era of climate change. Curr. Issue Tour. 18, 913–930.
Shih, W.M., Lin, T.P., Tan, N.X., Liu, M.H., 2017. Long-term perceptions of outdoor thermal environments in an elementary school in a hot-humid climate. Int. J. Biometeorol. 61, 1657–1666.
Shiue, I., Matzarakis, A., 2011. Estimation of the tourism climate in the Hunter Region, Australia, in the early twenty-first century. Int. J. Biometeorol. 55, 565–574.
Skelhorn, C., Lindley, S., Levermore, G., 2014. The impact of vegetation types on air and surface temperatures in a temperate city: a fine scale assessment in Manchester, UK. Landsc. Urban Plan. 121, 129–140.
Srivanit, M., Hokao, K., 2013. Evaluating the cooling effects of greening for improving the outdoor thermal environment at an institutional campus in the summer. Build. Environ. 66, 158–172.
Taleb, D., Abu-Hijleh, B., 2013. Urban heat islands: potential effect of organic and structured urban configurations on temperature variations in Dubai, UAE. Renew. Energy 50, 747–762.
Taleb, H., Taleb, D., 2014. Enhancing the thermal comfort on urban level in a desert area: case study of Dubai, United Arab Emirates. Urban For. Urban Green. 13, 253–260.
Taleghani, M., Sailor, D.J., Tenpierik, M., van den Dobbelsteen, A., 2014. Thermal assessment of heat mitigation strategies: the case of Portland State University, Oregon, USA. Build. Environ. 73, 138–150.
Taleghani, M., Kleerekoper, L., Tenpierik, M., van den Dobbelsteen, A., 2015. Outdoor thermal comfort within five different urban forms in the Netherlands. Build. Environ. 83, 65–78.
UNDRO, 1980. Natural disasters and vulnerability analysis. Report of Experts Group Meeting of 9–12 July 1979. UNDRO, Geneva, Switzerland.
UNISDR, 2004. Living With Risk. United Nations International Strategy for Disaster Reduction, Geneva, Switzerland.
VDI, 1998. Methods for the human biometeorological evaluation of climate and air quality for the urban and regional planning. Part I: Climate. VDI Guideline 3787. Part 2. Beuth, Berlin.
Wang, Y.P., Akbari, H., 2014. Effect of sky view factor on outdoor temperature and comfort in Montreal. Environ. Eng. Sci. 31, 272–287.
Wang, Y.P., Zacharias, J., 2015. Landscape modification for ambient environmental improvement in central business districts - a case from Beijing. Urban For. Urban Green. 14, 8–18.
Wang, X., Chen, D., Ren, Z., 2010. Assessment of climate change impact on residential building heating and cooling energy requirement in Australia. Build. Environ. 45, 1663–1682.
Wania, A., Bruse, M., Blond, N., Weber, C., 2012. Analysing the influence of different street vegetation on traffic-induced particle dispersion using microscale simulations. J. Environ. Manag. 94, 91–101.
Watson, I.D., Johnson, G.T., 1987. Graphical estimation of sky view-factors in urban environments. J. Climatol. 7, 193–197.
Yang, S.R., Lin, T.P., 2016. An integrated outdoor spaces design procedure to relieve heat stress in hot and humid regions. Build. Environ. 99, 149–160.
Yang, W., Wong, N.H., Zhang, G.Q., 2013a. A comparative analysis of human thermal conditions in outdoor urban spaces in the summer season in Singapore and Changsha, China. Int. J. Biometeorol. 57, 895–907.
Yang, X.S., Zhao, L.H., Bruse, M., Meng, Q.L., 2013b. Evaluation of a microclimate model for predicting the thermal behavior of different ground surfaces. Build. Environ. 60, 93–104.
Yang, J.C., Wang, Z.H., Kaloush, K.E., 2015. Environmental impacts of reflective materials: is high albedo a 'silver bullet' for mitigating urban heat island? Renew. Sust. Energ. Rev. 47, 830–843.
Yin, J.F., Zheng, Y.F., Wu, R.J., Tan, J.G., Ye, D.X., Wang, W., 2012. An analysis of influential factors on outdoor thermal comfort in summer. Int. J. Biometeorol. 56, 941–948.